CANCER BIOLOGY & THERAPY
2024, VOL. 25, NO. 1, 2360768
https://doi.org/10.1080/15384047.2024.2360768

Taylor & Francis
Taylor & Francis Group

RESEARCH PAPER

Circ_RPPH1 facilitates progression of breast cancer via miR-1296-5p/TRIM14 axis

Jing Jiang, Shenghong Shi, Wei Zhang, Chao Li, Long Sun, Qidong Ge, and Xujun Li

Department of Breast Surgery, Ningbo, Zhejiang, China

ABSTRACT

Circular RNA Ribonuclease P RNA Component H1 (*circ_RPPH1*) and microRNA (miRNA) *miR-1296-5p* play a crucial role in breast cancer (BC), but the molecular mechanism is vague. Evidence showed that *miR-1296-5p* can activate *tripartite motif-containing 14* (*TRIM14*). Clinical indications of eighty BC patients were collected and the *circ_RPPH1* expression was detected using real-time quantitative PCR. MCF-7 and MDA-MB-231 cells were transfected with overexpression or knockdown of *circ_RPPH1*, *miR-1296-5p*, or *TRIM14*. Cell counting kit-8, cell cloning formation, wound healing, Transwell, and flow cytometry assays were performed to investigate the malignant phenotype of BC. The dual-luciferase reporter gene analyses were applied to reveal the interaction between these target genes. Subcutaneous tumorigenic model mice were established with *circ_RPPH1* overexpression MDA-MB-231 cells in vivo; the tumor weight and volume, levels of *miR-1296-5* and *TRIM14* mRNA were measured. Western blot and immunohistochemistry were used to detect TRIM14 in cells and mice. *Circ_RPPH1* levels were notably higher in BC patients and have been found to promote cell proliferation, invasion, and migration of BC cells. *Circ_RPPH1* altered cell cycle and hindered apoptosis. *Circ_RPPH1* knockdown or *miR-1296-5p* overexpression inhibited the malignant phenotype of BC. Furthermore, *miR-1296-5p* knockdown reversed *circ_RPPH1*'s promotion effects on BC. Interestingly, *TRIM14* overexpression counteracts the inhibitory effects of *miR-1296-5p* overexpression and *circ_RPPH1* silencing on BC. Moreover, in BC tumor-bearing mice, *circ_RPPH1* overexpression led to increased TRIM14 expression and facilitated tumor growth. *Circ_RPPH1* enhanced BC progression through *miR-1296-5p/TRIM14* axis, indicating its potential as a biomarker and therapeutic target in BC.

ARTICLE HISTORY
Received 18 December 2023
Revised 14 May 2024
Accepted 23 May 2024

KEYWORDS
Breast cancer; circular RNA ribonuclease P RNA component H1; microRNA-1296-5p; tripartite motif-containing 14

1. Introduction

Breast cancer (BC) is a malignant tumor in women worldwide,[1] and has become a major threat to the life health of women. Due to its high morbidity and mortality rates, 2.26 million women have been affected with BC in 2020[2] and there are 1.7 million new incidences every year.[3] BC is diagnosed by breast self-examination and clinical breast examination,[4] and mammography or ultrasonography is used for BC screening.[5,6] The Tumor-Node-Metastasis (TNM)-based staging of BC represents different severity of BC, the larger number is on behalf of the more serious BC.[7] In recent years, surgery, endocrine drugs, or targeted drug therapy[8] and radiotherapy[9] have been performed in BC treatment. In addition, because of triple-negative BC, endocrine therapy brings little effect.[10] So, the mechanism of BC remains to be further studied and elucidated. Therefore, we need to pay more attention to studying the biomarkers and the potential mechanisms in BC.

Circular RNA (circRNA) Ribonuclease P RNA Component H1 (*circ_RPPH1*) is a highly expressed circRNA in BC. Evidence shown that circ_RPPH1 has a higher expression level in BC tissues compared to adjacent tissues.[11,12] Studies have shown that *circ_RPPH1* knockout delays tumor deterioration in BC.[13] Evidence has shown that circRNA plays a crucial role in malignant tumors through microRNAs (miRNAs) as a sponge.[14] *Circ_RPPH1* sponges *miR-296-5p* and *miR-146b-3p* to promote BC[15,16] suggesting that *circ_RPPH1* has a crucial role in regulating BC as a miRNA sponge.

MiRNAs play crucial roles in proliferation, migration, invasion and metastasis of BC cells.[17,18] Among them, miR-1296-5p has drawn considerable attention in recent years. *MiR-1296-5p* shows low expression in BC tissues and cells, and overexpression of *miR-1296-5p* inhibits BC malignant phenotype.[19] Moreover, *miR-1296-5p* promotes the sensitivity of BC cells to cisplatin and 5-fluorouracil.[20] *Tripartite motif-containing (TRIM) 14* was a downstream target of *miR-1296-5p*, and *circ_0048764* can activate the *TRIM14* in BC cells by targeting *miR-1296-5p*.[21] Although several studies of circRNA-miRNA-mRNA regulatory axis in BC have been done, how *circ_RPPH1* regulates the *miR-1296-5p*/*TRIM14* axis is still unclear. Here, we find that *circ_RPPH1* is elevated in BC and the clinical indications expression is related to increased *circ_RPPH1* in BC patients. Additionally, we suspect that circRNAs could promote tumor progression of BC by inhibiting *miR-1296-5p*. We performed lentivirus or plasmid transfection on BC cells to study the effects of *circ_RPPH1* on BC promotion and the mechanism of *circ_RPPH1* on activating *TRIM14* through inhibiting *miR-1296-5p*. Subcutaneous tumorigenic model mice were established with BC

CONTACT Xujun Li 13165903056@163.com Department of Breast Surgery, Ningbo No. 2 Hospital, No. 41, Xibei Street, Haishu District, Ningbo, Zhejiang 315000, China

Supplemental data for this article can be accessed online at https://doi.org/10.1080/15384047.2024.2360768

subcutaneous tumors to verify the mechanism of *circ_RPPH1* on BC tumor Growth.

2. Results

2.1. The increased circ_RPPH1 expression in tumor tissues of BC patients

We used UALCAN database to analyze the *circ_RPPH1* expression in breast invasive carcinoma (BRCA) from TGCA. The *circ_RPPH1* expression is increased in primary tumor group compared to the normal group, with a statistical significance (Supplementary figure S1). The *circ_RPPH1* expression in BC tissues of patients was detected using real-time quantitative PCR (RT-qPCR) (Figure 1(a)). The mRNA expression of *circ_RPPH1* in BC tissues was higher than in pa-carcinoma tissues. A chi-square test was performed to examine the difference in frequency distribution. Results are as shown in Table 1. The frequency distribution differences of high and low *circ_RPPH1* expression was significantly different in TNM staging. Additionally, there was no significant difference in age, tumor size, pausimenia or not, lymph node metastasis (N1) or not (N0), ER, PR, HER2.

2.2. Circ_RPPH1 promotes cell mobility and inhibits cell apoptosis in BC cells

The circ_RPPH1 overexpression [*circ_RPPH1* (+)] cells were successfully established (supplementary figure S2a). In Figure 1(b,c), cell viability in *circ_RPPH1* (+) group was increased. To further study the mechanisms of *circ_RPPH1* on BC cell mobility, cell cloning formation, wound healing and Transwell assays were performed. Figure 1(d,e) showed that *circ_RPPH1* increased the number of colonies in BC cells. In Figure 1(f,g), the cell migration of both cells was increased by *circ_RPPH1*. Moreover, in Figure 1(h,i), *circ_RPPH1* elevated the number of invaded cells. These results indicated that *circ_RPPH1* promoted the cell reproductive capacity, cell migration capacity and cell invasion capacity of BC cells.

Compared to negative control (NC) group, *circ_RPPH1* (+) group had a significantly decreased percentage of G0/G1 and G2/M cells, and cells in the S phase were accordingly increased (Figure 2(a-c)). From the results of flow cytometry (FCM) in Figure 2(d,e), *circ_RPPH1* overexpressing inhibited the BC cell apoptosis rate. Additionally, Western blot was used to measure TRIM14 protein expression and showed that TRIM14 protein expression was increased in circ_RPPH1 (+) groups (Figure 2(f)).

2.3. Circ_RPPH1 promotes cell mobility and inhibits cell apoptosis in BC cells by inhibiting miR-1296-5p

Figure 3(a) revealed the predicted results of the binding situation of circ_RPPH1 and *miR-1296-5p* that the target sequence of *miR-1296-5p* was located at 23–29 bp of *circ_RPPH1* gene 3'-UTR. In Figure 3(b), in the *circ_RPPH1* WT, compared with the NC group, the luciferase activity in the *miR-1296-5p* group was decreased. There was no significant difference between the NC group and the *miR-1296-5p* group in the *circ_RPPH1* mutant (Mut). These findings confirmed that *circ_RPPH1* is directly bound to miR-1296-5p. From the RT-qPCR verification results in Figure 3(c,d), *circ_RPPH1* and *miR-1296-5p* levels were reduced after transfection, indicating successful transfection.

Circ_RPPH1 (-) inhibited the cell viability of BC cells while the *miR-1296-5p* (-) reversed the tendency and promoted the cell viability in Figure 3(e,f). Similarly, Figure 3(g,h) showed that *circ_RPPH1* (-) reduced the number of colonies in BC cells and *miR-1296-5p* (-) increased it. The cell wound healing assay (Figure 3(i,j)) and Transwell assay (Figure 3(k,l)) also indicated similar results. In Figure 4(a-c), *circ_RPPH1* (-) increased the cells in G0/G1 significantly and reduced the cells in the G2/M which indicated that cells were blocked in the G0/G1, while all changes induced by *circ_RPPH1* (-) in cell cycle were reversed by *miR-1296-5p* (-). Furthermore, *circ_RPPH1* (-) promoted the cell apoptosis while *miR-1296-5p* (-) reversed it in Figure 4(d,e). Moreover, Western blot assay showed that TRIM14 protein expression was decreased in MCF-7 and MDA-MB-231 cells with circ_RPPH1 overexpression (Figure 4(f)). This was antagonized by miR-1296-5p knockdown (Figure 4(f)).

2.4. The interaction between miR-1296-5p and TRIM14 affects the cell mobility, cell cycles and inhibits cell apoptosis in BC cells

MiR-1296-5p overexpression [*miR-1296-5p* (+)] and *TRIM14* overexpression [*TRIM14* (+)] cells were established (supplementary figure S2b, c). Figure 5(a) revealed the binding situation of *miR-1296-5p* and *TRIM14* that the target sequence of *miR-12966-5p* was located at 187–194 bp of *TRIM14* gene 3'-UTR. In Figure 5 (b), in the TRIM14 WT, the luciferase detection of the *miR-1296-5p* group was decreased. In the TRIM14 Mut, there was no significant difference between the NC and *miR-1296-5p* groups.

MiR-1296-5p (+) inhibited the cell viability of BC cells, while the *miR-1296-5p* (+) cells with *TRIM14* (+) treatment increased the cell viability inversely (Figure 5(c,d)). In addition, *miR-1296-5p* (+) had similar effects of *circ_RPPH1* (-) on BC cell malignant phenotype (Figure 5(e-j)) to inhibit proliferation, migration, and invasion of BC cells, while TRIM14 (+) reversed it. The FCM was used to evaluate cell cycle and apoptosis, and the results were revealed in Figure 6 (a-e). It was found that GO/G1 cell percentage and cell apoptosis in BC were markedly increased by *miR-1296-5p* (+) treatment, which were reversed by TRIM14 (+) (Figure 6(a-e)). Results of Western bolt (Figure 6(f-i)) showed that *miR-1296-5p* (+) decreased the expression of TRIM14, while *TRIM14* (+) reversed *miR-1296-5p* (+) effects.

2.5. TRIM14 overexpression promotes the cell viability and migration in BC cells with circ_RPPH1 silencing

To clarify that *TRIM14* acts as a molecule of *circ_RPPH1*-regulated the malignant phenotype of BC cells, TRIM14 gene and proteins were increased in BC cells with *circ_RPPH1* (-) silencing (Supplementary figure S3a). Cell counting kit-8 (CCK-8) and cell wound healing assay were used. TRIM14

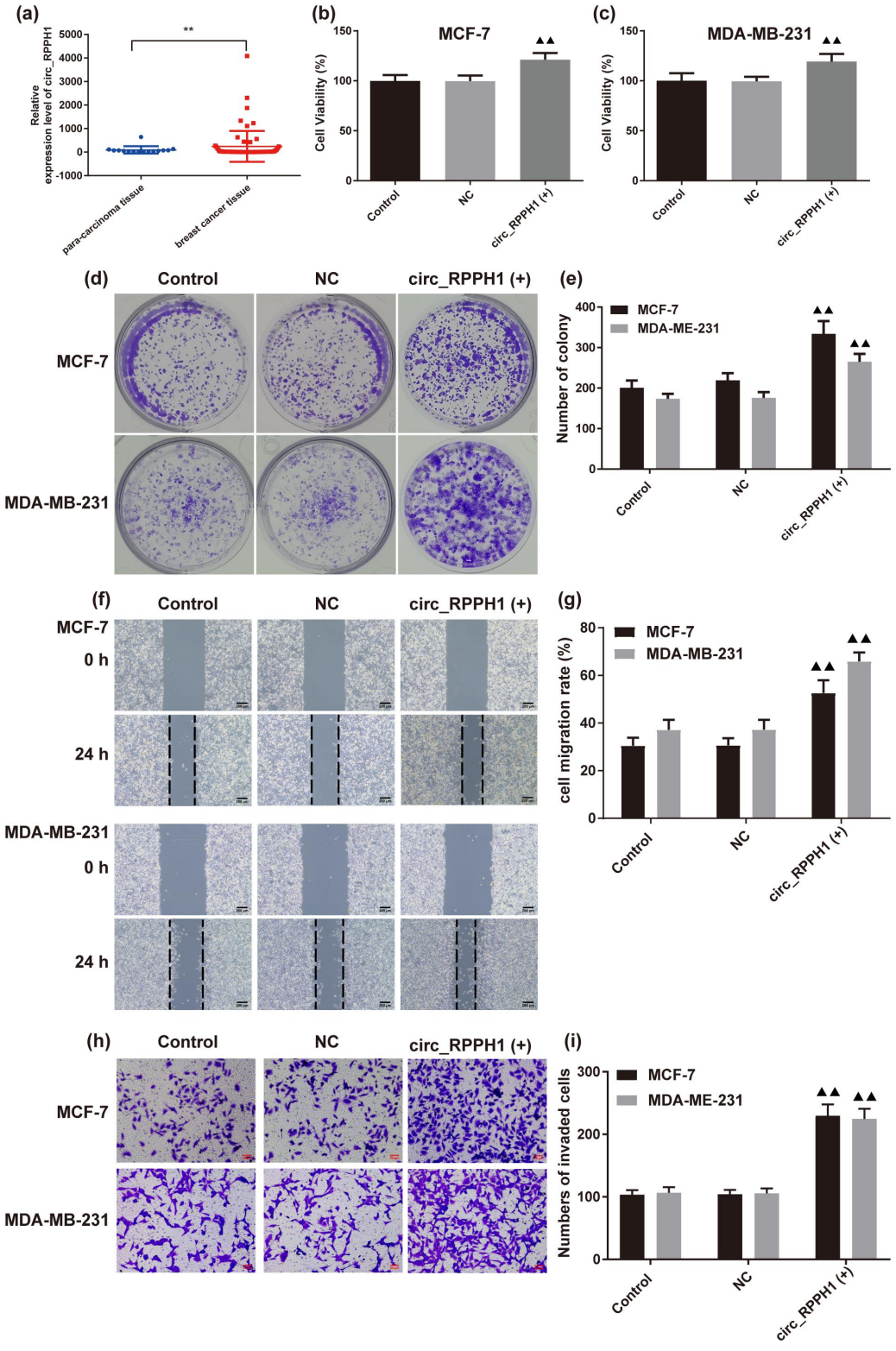

Figure 1. *Circ_RPPH1* overexpression promoted malignant phenotype of BC cells. (a) Real-time quantitative PCR (RT-qPCR) was used to detect *circ_RPPH1* expression in patients with BC; *circ_RPPH1* mRNA expression in BC tissues was higher than in para-carcinoma tissues ($n = 80$). (b-c) Cell counting kit-8 assay was used to measure the cell viability of BC cells; *circ_RPPH1* overexpression [*circ_RPPH1*(+)] increased cell viability of MCF-7 cells and MDA-MB-231 cells ($n = 6$). The cell viability (%) = (OD_{450} of the experimental group − average OD_{450} of the blank group)/(average OD_{450} of the Control group − average OD_{450} of the blank group) × 100%. (d-e) Cell cloning formation assay was used to detect the proliferation of BC cells; *circ_RPPH1* (+) promoted proliferation of MCF-7 cells and MDA-MB-231 cells ($n = 3$). (f-g) Cell wound healing assay was used for cell migration detection; *circ_RPPH1* (+) promoted migration of MCF-7 cells and MDA-MB-231 cells ($n = 3$, scale bar = 200 μm). The cell migration rate (%) = (0 h scratch width −24 h scratch width)/0 h scratch width × 100%. (h-i) Transwell assay was used to detect the invasion of BC cells; *circ_RPPH1* (+) promoted invasion of MCF-7 cells and MDA-MB-231 cells ($n = 3$, scale bar = 50 μm). Data were presented as the mean ± SD. $^{**}p < .01$ *vs*. the para-carcinoma tissue; $^{▲▲}p < .01$ *vs*. the Control group.

Table 1. Correlation analysis between clinical indications and circ_RPPH1 expression in clinical BC samples ($n = 80$).

Elements	Group (numbers)	*circ_RPPH1* expression		Probability Value (p value)
		High expression ($n = 33$)	Low expression ($n = 32$)	
Age	≥50 ($n = 49$)	19	21	.505
	<50 ($n = 25$)	14	11	
Tumor size	≥2 cm ($n = 42$)	20	22	.492
	<2 cm ($n = 23$)	13	10	
Pausimenia or not	Menopause ($n = 39$)	20	19	.919
	No menopause ($n = 26$)	13	13	
TNM staging	I + II ($n = 55$)	23	22	**.003**
	III ($n = 10$)	10	0	
Lymph node metastasis (N1) or not (N0)	N1 ($n = 29$)	18	11	.102
	N0 ($n = 36$)	15	21	
Estrogen receptor (ER)	Negative ($n = 20$)	10	10	.934
	Positive ($n = 45$)	23	22	
Progesterone receptor (PR)	Negative ($n = 26$)	13	13	.919
	Positive ($n = 39$)	20	19	
Human epidermal growth factor receptor (HER2)	Negative ($n = 52$)	27	25	.710
	Positive ($n = 13$)	6	7	

overexpression was found to promote the cell viability and migration rats in BC cells with circ_RPPH1 silencing (Supplementary figure S3b,c).

2.6. Circ_RPPH1 promotes tumor progression of BC in mice

In Figure 7(a-c), the *circ_RPPH1* (+) promoted the size and weight of BC in mice. The RT-qPCR results in Figure 7(d,e) revealed that *circ_RPPH1* (+) decreased the mRNA expression of *miR-1296-5p* and increased *TRIM14* expression. The results in the IHC and Western blot (Figure 7(f-g)) showed TRIM14 expression in BC tumor and found that *circ_RPPH1* (+) increased TRIM14 expression levels.

3. Discussion

At present, *circ_RPPH1* plays an important role in BC pathogenesis[16,22] and is helpful for BC diagnosis and treatment. CircRNAs up-regulated the expression of TRIM14 via targeting *miR-1296-5p* to promote BC growth.[21] By examining the *circ_RPPH1* level in 80 BC tissues of patients, we validated that the *circ_RPPH1* level was highly expressed in BC tissues. It was expected to become a potential biomarker and target of BC. Our study confirmed the high expression of *circ_RPPH1* in BC, and *circ_RPPH1* promoted *TRIM14* by inhibiting *miR-1296-5p* to facilitate BC progression.

BC is a significant threat to women's lives and health. Although most women have heard of BC and about half are aware of the risk factors for BC, not all women are knowledgeable about BC warning signs or symptoms.[23] In this study, clinical BC samples from female patients of different ages showed that *circ_RPPH1* expression distribution was different in the TNM staging. The *in vitro* study verified the high expression of circ_RPPH1 in BC cells. Circ_RPPH1 promoted the tumor growth of BC *in vivo*. This indicated that circ_RPPH1 was important in BC progression and may serve as a biomarker for disease diagnosis of BC.

Research has shown that circRNAs function through competing endogenous RNA (ceRNA) in BC cell mobility.[24] *Circ_RPPH1* was conducted as ceRNA to reduce the inhibitory roles of miR-146b-3p on E2F2 to promote BC.[16] Circ_RPPH1 knockdown restrained glioma growth through binding to miR-627-5p/miR-663a.[25] Moreover, *circ_RPPH1* accelerated the aggravation of BC by miR-542-3p/ARHGAP1 axis.[22] In this study, *circ_RPPH1* affected *miR-1296-5p* through the ceRNA to regulate *TRIM14* and the BC cell mobility had a significant promotion. Therole of *miR-1296-5p* in BC is still ambiguous, *miR-1296-5p* was reported to inhibit the gastric cancer via regulating EGFR and CDK6.[26] Moreover, *miR-1296-5p* also inhibited the growth of human osteosarcoma by regulating notch receptor 2.[27] *TRIM14* is highly expressed in tumors, including gastric cancer,[28] tongue cancer,[29] glioma[30] and BC,[31] etc. Our study confirmed that *TRIM14* was a target for *miR-1296-5p*. We prove that *miR-1296-5p* plays an antineoplastic role in BC and *circ_RPPH1/miR-1296-5p* knockdown promotes tumor progression in BC by activating *TRIM14*, suggesting that the promoting effect in BC of *circ_RPPH1* was involved in regulating the *miR-1296-5p*/*TRIM14* axis.

However, our study has some limitations, including the combination mode of *circ_RPPH1* and *miR-1296-5p*. Additionally, if the effects of silencing miR-296-5p and overexpressing TRIM14 in BC cells can be detected separately, the evidence chain of this study will be more complete. In the future, we will probe the effects and mechanisms of *circ_RPPH1* in BC in more detail. Moreover, the further study of the circRNA-miRNA-mRNA axis in BC will help the establishment of BC regulatory network and strengthen the mechanism study on anti-BC.

4. Conclusion

In conclusion, *circ_RPPH1* promoted the proliferation, invasion, and migration of BC by inhibiting *miR-1296-5p* and thereby up-regulating TRIM14. Animal experiments confirmed that the oncogenic role of *circ_RPPH1* overexpression in BC progression. *Circ_RPPH1* could be used as a promising biomarker and therapeutic target for study and treatment of BC.

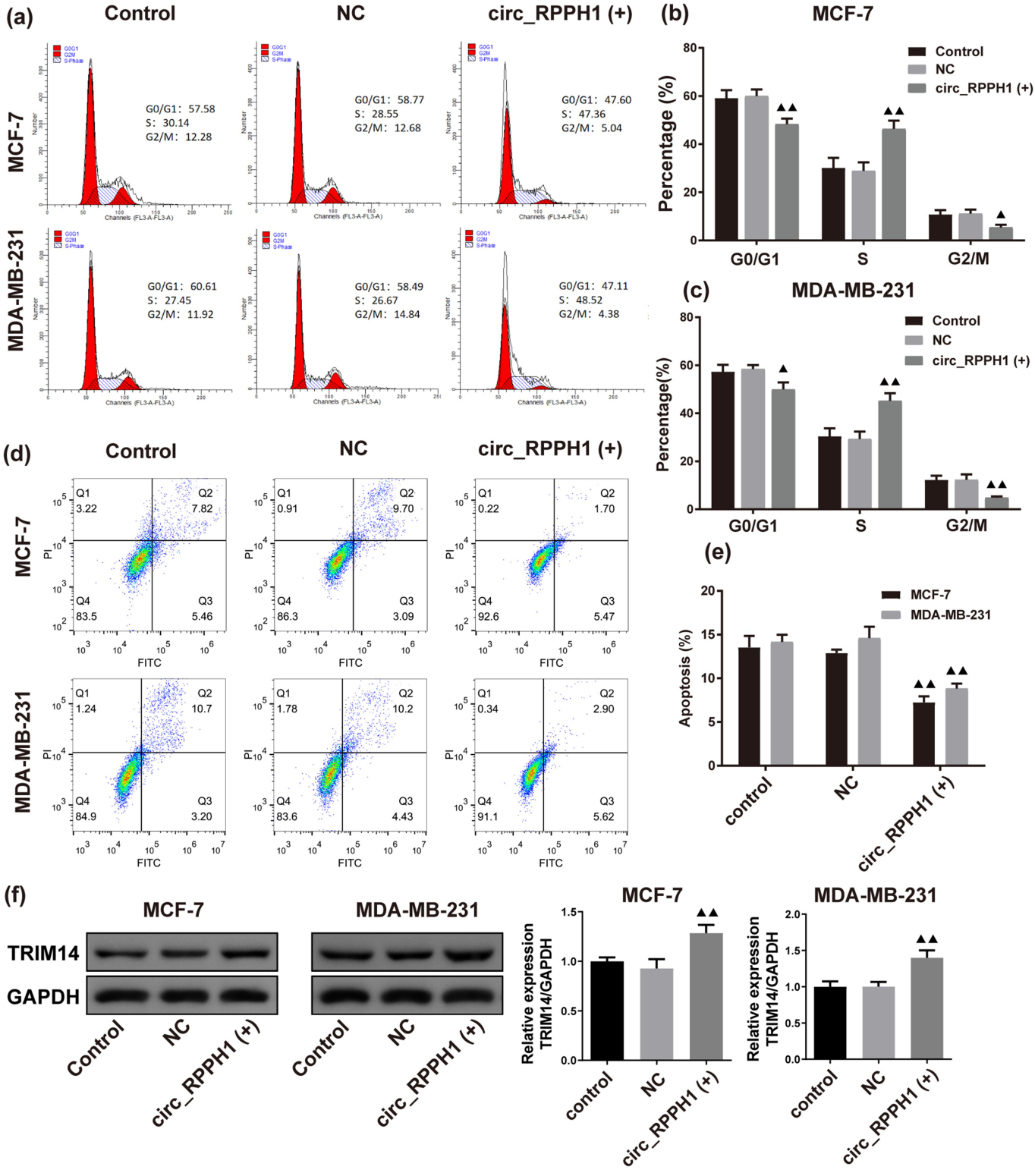

Figure 2. *Circ_RPPH1* overexpression promoted BC cell entry into S phase and inhibited cell apoptosis. (a-c) Flow cytometry was used to detect the cycle of BC cells; *circ_RPPH1* overexpression [*circ_RPPH1*(+)] decreased cells in the G0/G1 and G2/M phase, as well as promoting cells entry into the S phase in MCF-7 cells and MDA-MB -231 cells. (d-e) Flow cytometry was also used to detect the apoptosis; *circ_RPPH1* (+) inhibited apoptosis in MCF-7 cells and MDA-MB-231 cells. (f) Western blot assay was used to detect TRIM14 protein expression. *Circ_RPPH1* (+) increased TRIM14 protein expression in MCF-7 and MDA-MB-231 cells. Data were presented as the mean ± SD, $n = 3$. ▲▲$p < .01$ *vs*. the Control group.

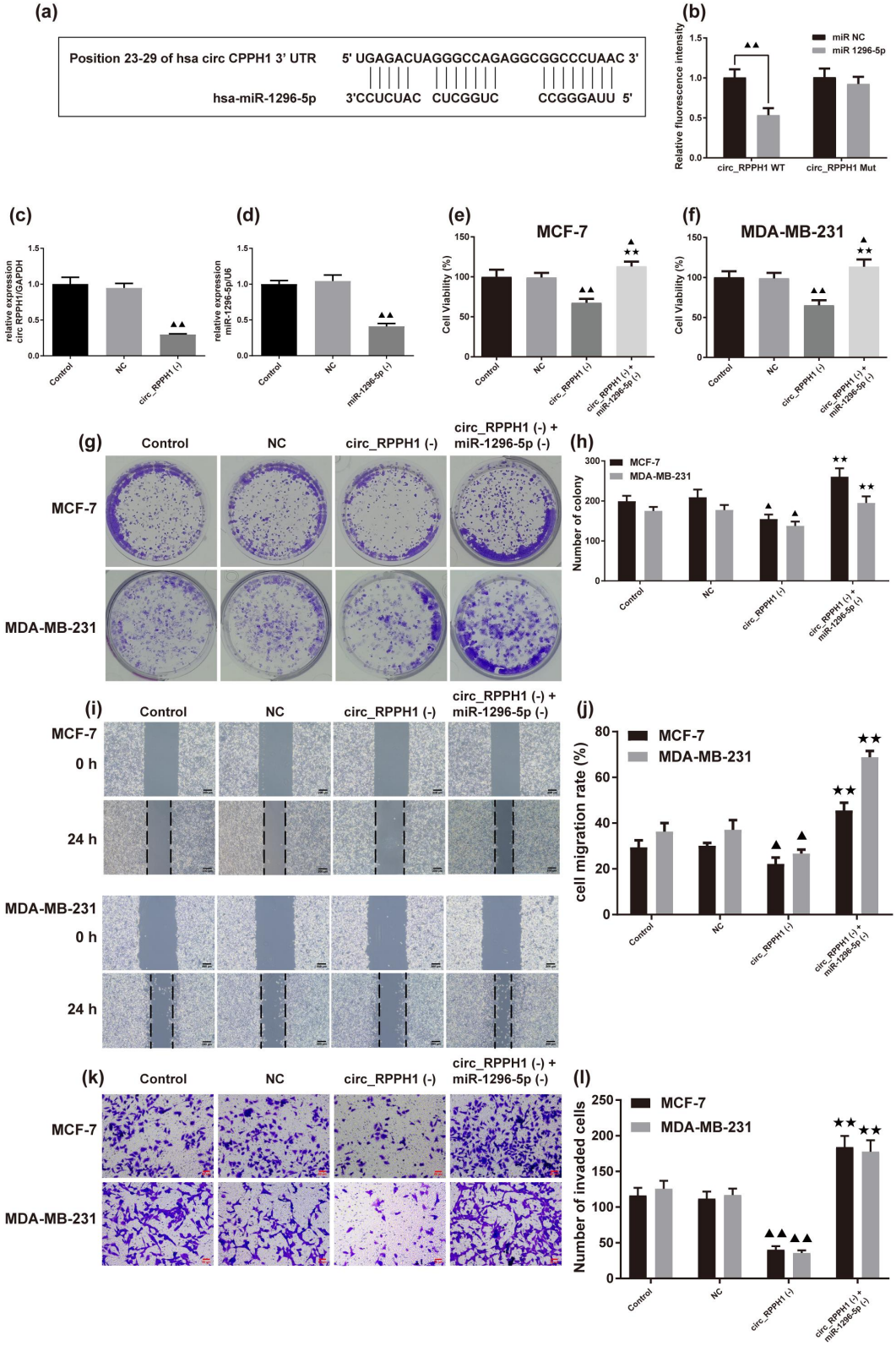

Figure 3. *Circ_RPPH1* silencing inhibited BC cell malignant phenotype by increasing *miR-1296-5p*. (a) The predicted results of the binding situation of *circ_RPPH1* and *miR-1296-5p*. (b) The luciferase activities in BC cells co-transferred with wild-type (WT) or mutant (Mut) *circ_RPPH1* plasmid together with miR-1296-5p mimic or mic-NC ($n = 3$). (c-d) Results of RT-qPCR verified the silencing of *circ_RPPH1* [*circ_RPPH1*(-)] and *miR-1296-5p* [*miR-1296-5* (-)] in BC cells ($n = 3$). (e-f) *Circ_RPPH1* (-) inhibited cell viability, while *miR-1296-5p* (-) treatment reversed it ($n = 6$). (g, h) Results of cell cloning formation assay; (i, j) Results of wound healing assay; (k, l) Results of Transwell assay; they respectively revealed the inhibitory effects of *circ_RPPH1* (-) on BC cell proliferation, migration, and invasion, while *miR-1296-5p* (-) treatment reversed it ($n = 3$, scale bar = 200 μm or 50 μm). Data were presented as the mean ± SD. ▲$p < .05$, ▲▲$p < .01$ *vs*. the Control group; ★$p < .05$, ★★$p < .01$ *vs*. the *circ_RPPH1* silencing (-) group.

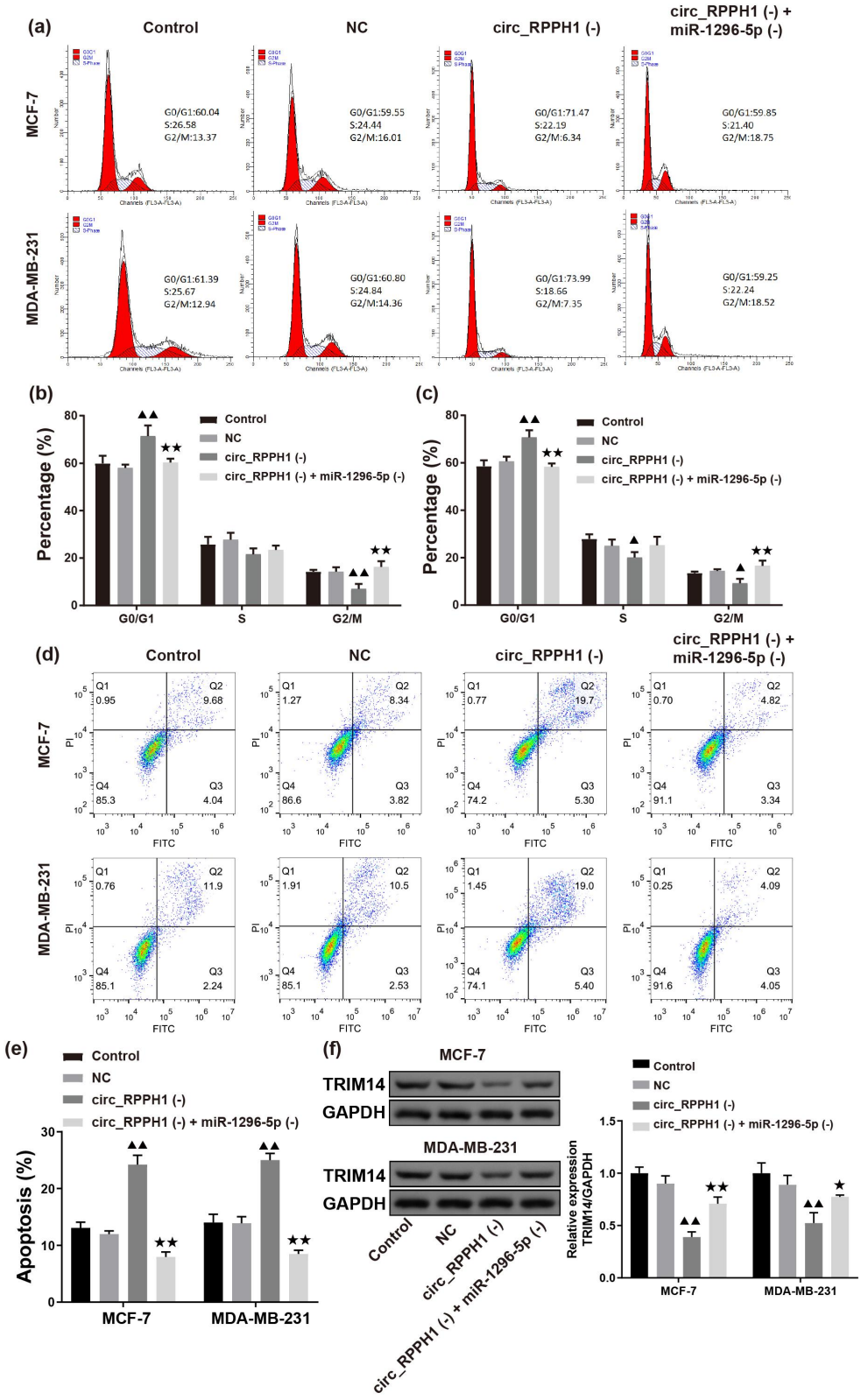

Figure 4. *Circ_RPPH1* silencing blocked the G0/G1 phase and inhibited apoptosis in BC cells by increasing *miR-1296-5p*. (a-c) the effects of *circ_RPPH1* silencing [*circ_RPPH1*(-)] and *miR-1296-5p* silencing [*circ_RPPH1*(-)] of the cell cycle in BC cells. *Circ_RPPH1* silencing blocked the G0/G1 phase. (d-e) *Circ_RPPH1* (-) promoted apoptosis in BC cells, but *miR-1296-5p* (-) reversed it. (f) Western blot assay was used to detect TRIM14 protein expression. *Circ_RPPH1* (-) inhibited TRIM14 protein expression in MCF-7 and MDA-MB-231 cells, while *mir-1296-5p* (-) antagonized this. Data were presented as the mean ± SD, $n = 3$. ▲$p < .05$, ▲▲$p < .01$ *vs*. the Control group; ★★$p < .01$ *vs*. the *circ_RPPH1* (-) group.

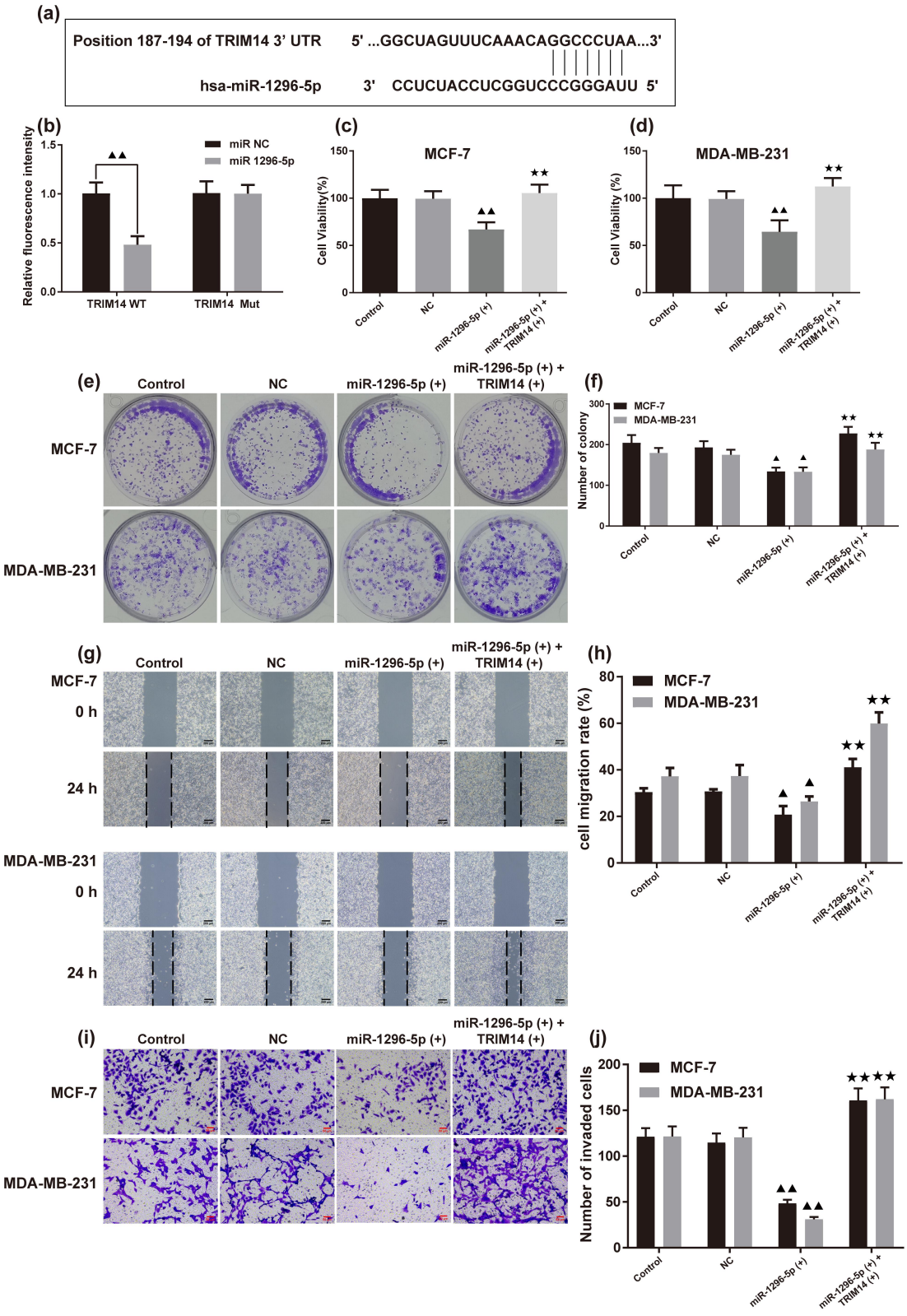

Figure 5. *MiR-1296-5p* overexpression inhibited BC cell malignant phenotype via *TRIM14*. (a) The predicted results of the binding situation of *miR-1296-5p* and *TRIM14*. (b) The luciferase activities in BC cells co-transferred with WT or Mut *TRIM14* plasmid together with *miR-1296-5p* mimic or mic-NC ($n = 3$). (c-d) the overexpressing *miR-1296-5p* [*miR-1296-5* (+)] in MCF-7 and MDA-MB-231 cells inhibited cell viability while the overexpressing *TRIM14* [*TRIM14* (+)] reversed it ($n = 6$). (e, f) Results of cell cloning formation assay; (g, h) Results of wound healing assay; (i, j) Results of Transwell assay; they were respectively revealed the inhibitory effects of *miR-1296-5* (+) on the proliferation, migration, and invasion of MCF-7 and MDA-MB-231 cells, as well as and *TRIM14* (+) reversed it ($n = 3$, scale bar = 200 μm or 50 μm). Data were presented as the mean ± SD. ▲$p < .05$, ▲▲$p < .01$ *vs*. the Control group; ★★$p < .01$ *vs*. the *miR-1296-5p* (+) group.

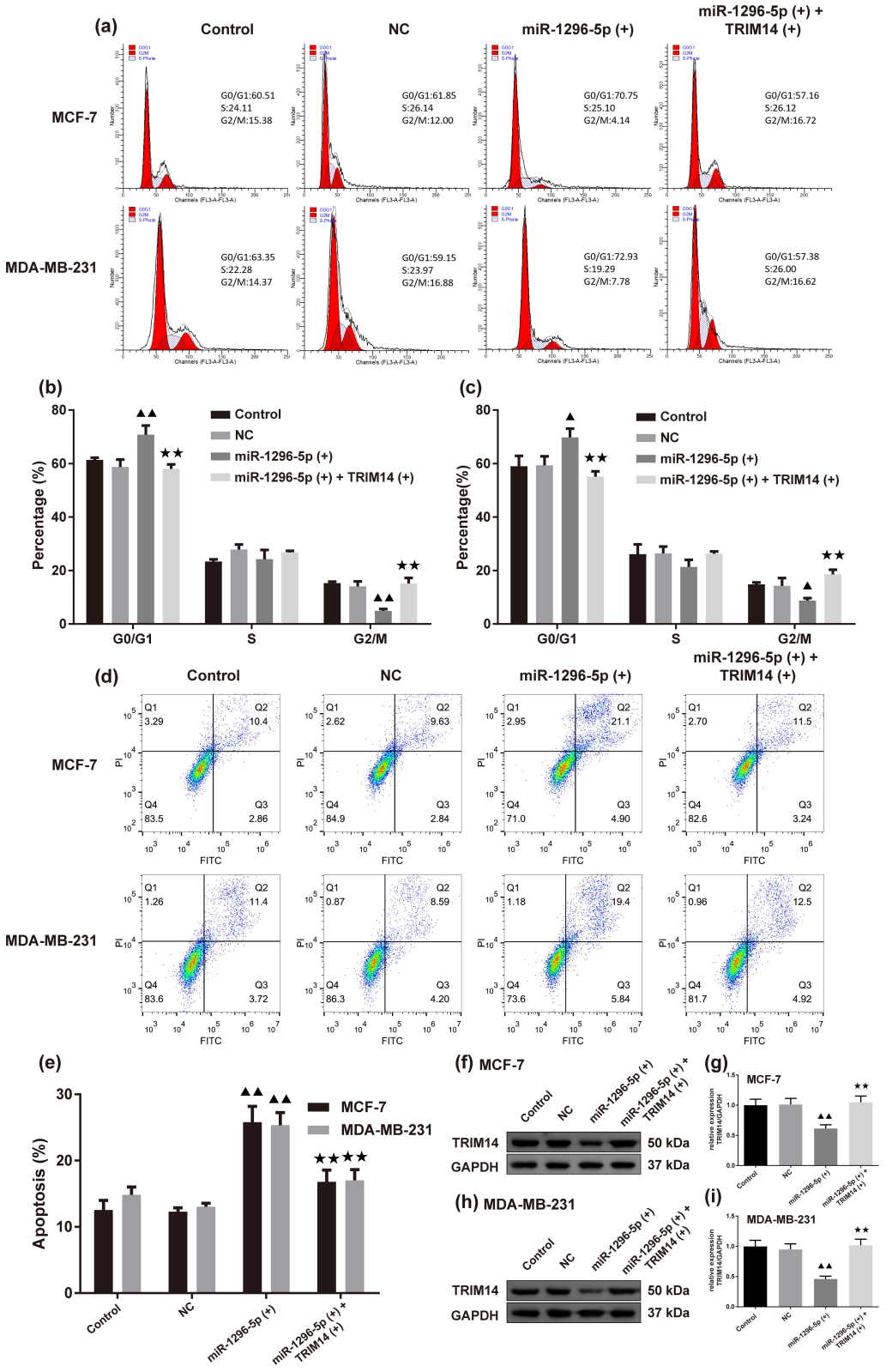

Figure 6. *MiR-1296-5p* overexpression blocked the G0/G1 phase and promoted apoptosis in BC cells. (a-c) Flow cytometry was used to detect the cycle of BC cells; The overexpressing *miR-1296-5p* [*miR-1296-5* (+)] increased percentage of GO/G1 cells in MCF-7 and MDA-MB-231 cells. (d-e) Flow cytometry was used to detect apoptosis of BC cells; *miR-1296-5* (+) promoted cell apoptosis. Overexpressing *TRIM14* [*TRIM14* (+)] reversed them. Data were presented as the mean ± SD, $n = 3$. $^{▲}p < .05$, $^{▲▲}p < .01$ *vs.* the Control group; $^{★★}p < .01$ *vs.* the *miR-1296-5p* (+) group.

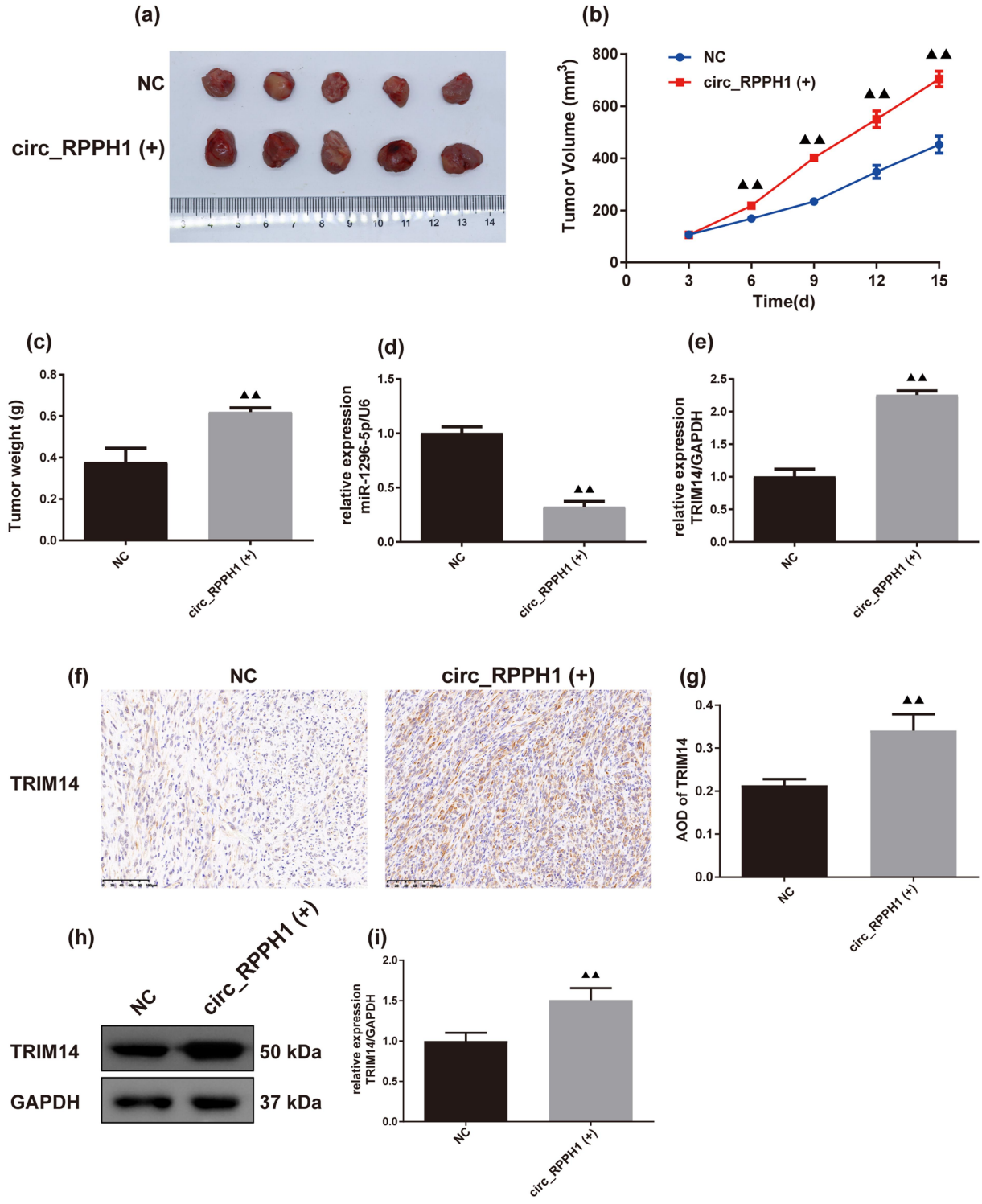

Figure 7. *Circ_RPPH1* overexpression promoted BC progression in mice. (a-c) the BC tumor size and weight in mice ($n = 5$). The tumor volume = length × width^2/2. (d, e) the levels of *miR-1296-5p* and *TRIM14* mRNA were detected by real-time quantitative PCR ($n = 3$). (f, g) Immunohistochemistry used to observe TRIM14 expression in BC tumor ($n = 3$, scale bar = 100 μm). (h, i) Western blot was used to detect TRIM14 expression levels in BC tumor. (h) Representative protein bands of TRIM14; (i) the semi-quantitative statistical analysis results of Western blot ($n = 3$). Data were presented as the mean ± SD. ▲▲$p < .01$ *vs*. the Control group. *circ_RPPH1*(+) group indicated *circ_RPPH1* overexpression group.

5. Material and methods

5.1. Clinical samples and analysis

UALCAN was used to analyze circ_RPPH1 expression in primary tumor of BRCA compared to the normal tissues (https://ualcan.path.uab.edu/cgi-bin/TCGAExResultNew2.pl?genenam=RPPH1&ctype=BRCA). BC ($n = 15$) and para-carcinoma ($n = 65$) tissues were collected from 80 patients recruited from Ningbo No.2 Hospital. The pa-carcinoma tissues are the adjacent normal tissues, and its isolation method refers to previous research.[32] Patients range in age from 28 to 84. Informed consent was obtained from

all patients. Ethics approval was obtained from Ningbo No.2 Hospital.

Clinical information was recorded by physicians using a standardized form, including the relation between circ_RPPH1 expression and clinical indications: age, tumor size, pausimenia or not, lymph node metastasis or not, TNM staging, estrogen receptor (ER), progesterone receptor (PR) as well as human epidermal growth factor receptor-2 (HER2).

5.2. Cell culture

MCF-7 cells and MDA-MB-231 cells are both human BC cells. MCF-7 cell lines (iCell-h129) and MDA-MB-231 cell lines (iCell-h133) were obtained from Shanghai iCell Bioscience Inc (China). MCF-7 cells were cultured in a DMEM medium containing 10% fetal bovine serum (FBS), and 1% penicillin-streptomycin solution and incubated in a cell incubator with a condition of 5% CO_2, 37°C. In addition, MDA-MB-231 cells were also cultured in the same medium but maintained air culturing without CO_2 to avoid cytotoxicity.

5.3. Lentivirus, small interfering RNA, and plasmid transfection and cell grouping

Vector lentivirus and circ_RPPH1 lentivirus were purchased from GeneChem (Shanghai, China). Briefly, the two BC cells (2×10^5 cells/well) were inoculated into 6-well plates and cultured until they reached 70–80% confluence. A complete medium containing virion and viral infection booster fluid was then used to infect cells for 24 h, followed by puromycin (ST551, Beyotime, China) selected for one week. *Circ_RPPH1*(GOSE0351480), *circ_RPPH1* small interfering RNA (siRNA) (GIDE0364124), *miR-1296-5p* siRNA (GMDE0364125), control siRNA (P22091400), plasmids encoding *miR-1296-5p* (GMUE0364119) or *TRIM14* cDNA (GOSE0364118) were purchased from GeneChem, Shanghai, China and were used to transfect cells for 6 h using a lipofectamine 3000 kit (L3000–008, Invitrogen, USA) according to the manufacturer's instructions. After transfection, fresh medium was replaced and cultured for 24 h.

Overexpression and knockdown of genes were indicated as (+) and (-), respectively. First, MCF-7 and MDA-MB-231 cells were divided into three groups: control, NC and *circ_RPPH1* (+) to evaluate the impact of *circ_RPPH1* overexpression on BC malignant phenotype. Additionally, four groups were created to analyze the inhibitory effects of *circ_RPPH1* knockdown on BC via *miR-1296-5p*: control, NC, *circ_RPPH1* silencing [*circ_RPPH1* (-)], and circ_RPPH1 (-) + *miR-1296-5p* silencing [*miR-1296-5p* (-)]. Moreover, to evaluate if *TRIM14* activation antagonizes the effects of *miR-1296-5p* overexpression on BC, these cells were divided into Control, NC, *miR-1296-5p* overexpression [*miR-1296-5p* (+)], and *miR-1296-5p* (+) + *TRIM14* overexpression [*TRIM14* (+)] groups. Additionally, *circ_RPPH1* (-) and *circ_RPPH1* (-) + *TRIM14* (+) groups were used to clarify that *TRIM14* is a downstream molecule of *circ_RPPH1* regulating cell viability and migration of BC cells.

5.4. Detection of luciferase activity

The 2×10^4 cells were seeded in 96-well plates for a dual-luciferase reporter gene assay. Luciferase was linked to *circ_RPPH1* wild-type (WT) and *circ_RPPH1* Mut or *TRIM14* WT and *TRIM14* Mut reporter vector or *miR-1296-5p* mimics or miR-NC, then transfected into MDA-MB-231 cells. After transfection, a dual-luciferase reporter gene assay system was applied. 20 μL collected cell lysate of groups was added in a black label plate. A firefly luciferase reaction fluid was added and mixed, followed by detecting the activity of firefly luciferase within 30 min at 550 nm. A Renilla luciferase reaction fluid was then added in each well and mixed, followed by detecting the activity of Renilla luciferase within 30 min at 480 nm.

5.5. Detection of the gene expression of circ_RPPH1, miR-1296-5p, and TRIM14

The gene expression of *circ_RPPH1*, *miR-1296-5p*, and *TRIM14* in BC human tissues, cells and mice tissues was examined using RT-qPCR. After a pre-processing of the samples, Buffer RLT, RNase-free ddH_2O and proteinase K solution were added to extract total RNA. The retro transcriptional response system was prepared for reverse transcriptional reaction. Then, a response system was prepared for Real-time fluorescence quantitative PCR reaction and carried out on the Roche LightCycler 96 RT-qPCR instrument (LightCycler® 96, Roche, Switzerland). GAPDH was the internal reference. The relative levels of target genes were measured by the $2^{-\Delta\Delta Ct}$. The primer sequences were shown in Table 2.

5.6. Detection of cell proliferation

The cell proliferation of BC cells was detected using CCK-8 and a cell cloning formation assay. For the CCK-8 assay, two cells were inoculated into 96-well plates of 2.5×10^3 cells/well and cultured in the cell incubator (37 °C) with their respective culture conditions for 24 h. Then, the lentiviral infection or plasmid transfection was performed for 6 h. The medium was

Table 2. The primer sequences.

Gene	Forward Primer	Reverse Primer
Human-*circ_RPPH1*	GGGAGGTGAGTTCCCAGAG	CAGGGAGAGCCCTGTTAGG
Human-*GAPDH*	GAATGGGCAGCCGTTAGGAA	AAAAGCATCACCCGGAGGAG
Human *miR-1296-5p*	GTTAGGGCCCTGGCTCC	CAGTGCGTGTCGTGGAGT
Mouse *TRIM14*	GTGCGTGTGCAGAAGCTAATC	CTGCGTAAACCTTGAGCCTTT
Mouse *GAPDH*	AGGTCGGTGTGAACGGATTTG	TGTAGACCATGTAGTTGAGGTCA

changed and cultured for 24 h again. 10 μL CCK-8 solution (C0039, Beyotime, China) was added and co-cultured for 2 h. The OD value was captured using a microplate reader (CMaxPlus, MD, USA) at 450 nm. For the cell cloning formation assay, the transfected cells were inoculated into 24-well plates of 2.5×10^5 cells/well. A DMEM medium containing 30% FBS was replaced the original medium. Every three days, the medium was changed. The clone size was observed under an optical microscope (AE2000, Motic, China). After two weeks, the cells were photographed. 4% paraformaldehyde was added to fix cells at 4°C for 1 h and followed by washing with PBS. Then, crystal violet dye was applied in wells to stain cells. Washed with PBS, the colony images were captured using a camera (850D, Canon Ltd., Japan). Finally, the colony number was counted microscopically.

5.7. Detection of cell migration

The cell migration capacity of BC cells was detected using a cell wound healing assay. The transfected cells were inoculated into 6-well plates of 5×10^5 cells/well and cultured in their respective culture conditions. When the cells were covered with the plates of 80%, a straight line was drawn evenly perpendicular to the bottom of the plate hole using a pipette tip. A serum-free medium was added for 24 h culture. The scratch was photographed using the optical microscope. Image J (Image-J, NIH, Germany) was used to analyze the cell migration rate.

5.8. Detection of cell invasion

The cell invasion of BC cells was detected using Transwell assay. The cells were resuspended to 2×10^4 cells/mL. Cell suspension containing 4×10^3 cells was added into the upper chamber of the Transwell chamber, and medium containing 10% FBS was added into the lower chamber, followed by culturing for 24 h in the cell incubator (37 °C). 4% paraformaldehyde was used to fix cells in lower chamber for 0.5 h. The crystal violet dye was used to stain cells. Finally, the cell images were photographed using the camera and the number of invaded cells was counted.

5.9. Detection of cell cycle

The FCM was applied to detect the cell cycle of BC cells. The infected or transfected cells were inoculated into 6-well plates of 5×10^5 cells/well. After 24 h culture, the cells were then collected and resuspended. DNA Staining solution (containing propidium iodide (PI) and RNase A 550,825, BD Pharmingen, USA) and permeabilization solution were added and co-incubated at 25°C for 30 min away from light. The cells were collected, and the cell cycle was detected using a flow cytometer (C6, BD, USA).

5.10. Detection of cell apoptosis

The cell apoptosis of BC cells was detected using FCM. After culture, the cell density was 1×10^6 cells/mL, and the binding buffer was added and mixed. Annexin V-FITC and PI were added for 15 min incubation away from light. Finally, the binding buffer was added again, and the flow cytometry was used for the detection of cell apoptosis rate within 60 min.

5.11. Subcutaneous tumorigenic model of BC cells in nude mice

Female BALB/c nude mice (8 weeks old, 18 g weight) were purchased from Beijing Vital River Laboratory Animal Technology Co., Ltd (China) of animal license permit No.: SCXK (Jing) 2016–0006. The nude mice were housed in the animal room with the SPF barrier system of Zhejiang Eyoung Pharmaceutical Research and Development Co., Ltd (China). The SPF animal room was under a 12-h dark/light cycle, room temperature of 23 ± 2°C and humidity of 60 ± 5%. All animal experiments were performed under the Experimental Animal Ethics Committee of Zhejiang Eyoung Pharmaceutical Research and Development Co., Ltd of License No. SYXK (Zhe) 2021–0033.

The nude mice were divided into two groups: NC and circ_RPPH1 overexpression [circ_RPPH1(+)]. MDA-MB-231 cells with circ_RPPH1 lentivirus and control lentivirus transfection were resuspended in normal saline. MDA-MB-231 cells (3×10^6 cells) were inoculated in the left axillary of each mouse. The tumor size was determined every three days. After 15 d of subcutaneous tumor injection, the mice were euthanized with CO_2, and the tumor tissues of mice were separated and weighed. The separated tumors were photographed.

5.12. Detection of the expression of TRIM14 in BC cells or tumor tissues in mice

Immunohistochemistry (IHC) and Western blot were performed to detect the level of TRIM14 in cells or tumor tissues. For the IHC assay of TRIM14, the paraffin-embed blocks of separated tumor tissues were cut into 5-μm sections. The sections were baked, dewaxed, and hydrated. Following by blocking with 3% H_2O_2 solution and repairing with boiling antigen repairing solution (1 mmol Tris-EDTA, pH = 9.0), 5% BSA was incubated with the sections for 20 min at 25°C. The primary antibody of TRIM14 (1:100, DF12490, Affinity, USA) diluted in antibody diluent was then added and co-incubated for 12 h at 4°C. The next day, the second antibody (1:5000, ab97080, Abcam, USA) diluted in antibody diluent was added and co-incubated for 0.5 h at 37°C. Following staining with DBA solution and hematoxylin dye, the sections were dehydrated and transparentized. Finally, neutral balsam was used to seal the sections and the IHC images were photographed using a microscope.

For the Western blot assay, the total protein in cells or tissues was extracted using Lysis buffer. A BCA kit was then used to measure the protein concentration and the protein concentration of each group was unified. 5 × loading buffer was added and boiled to degenerate protein. 10% SDS-PAGE was prepared, and the protein samples were added into the sample holes respectively and electrophoresed using an electrophoresis apparatus (EPS300, Tianneng, China). When the

protein entered the best separation part, transferred it to the PVDF membrane electrophoretically. The membrane was washed with TBST for 3 times and blocked with 5% skimmed milk powder. The membrane was then washed with TBST again and immediately transferred to primary antibodies of TRIM14 (1:1000), GAPDH (1:10000, AF7021, Affinity, USA) diluted in antibody diluent and co-incubated for 12 h at 4°C. The membrane was then washed and immediately co-incubated with the second antibody diluent (1:6000, #7074, Cell Signaling Technology, USA) for 90 min at 25°C. The membrane was washed and transferred into a chemiluminescence apparatus (610020-9Q, Shanghai Qinxiang Scientific Instrument Co., LTD, China) and ECL reagent was dropped on it. The protein band images were captured using chemi capture Software and analyzed using Image-J.

5.13. Statistical analysis

All the experiments above were repeated at least three times. SPSS 20.0 (SPSS, Chicago, USA) was used for data analysis. One-way analysis of variance (ANOVA) was used for quantitative data analysis, followed by Tukey's posttest with normal distribution data. When the distribution was normal, but the variance was not uniform, Dunnett's T3 test was used. All data were expressed as mean ± standard deviation (SD). $p < .05$ or $p < .01$ was defined as a significant difference between groups.

Acknowledgments

The authors greatly appreciate the efforts of all the authors.

Disclosure statement

No potential conflict of interest was reported by the author(s).

Funding

This work was supported by Ningbo Natural Science Foundation [2021J311] and the Project of Ningbo Leading Medical & Health Discipline [2022-B13].

ORCID

Xujun Li http://orcid.org/0009-0003-4552-5863

Authors' contributions

Conception and design of the research: Jing Jiang and Xujun Li
Acquisition of data: Qidong Ge and Long Sun
Analysis and interpretation of data: Jing Jiang and Shenghong Shi
Statistical analysis: Wei Zhang and Chao Li
Drafting the manuscript: Jing Jiang
Revision of the manuscript for important intellectual content: Jing Jiang and Xujun Li
Approval of final version of manuscript to be published: All authors
Agreement to be accountable for all aspects of the work ensuring that questions related to the accuracy or integrity of the work are appropriately investigated and resolved: Jing Jiang, Shenghong Shi, Wei Zhang, Chao Li, Long Sun, Qidong Ge and Xujun Li.

Data availability statement

The data presented in this study are available upon reasonable request from the corresponding author.

Ethics

Ethics approval was obtained from Ningbo No.2 Hospital in any experiment with human. All animal experiments were performed under the Experimental Animal Ethics Committee of Zhejiang Eyoung Pharmaceutical Research and Development Co., Ltd of License No. SYXK (Zhe) 2021–0033.

References

1. Barzaman K, Karami J, Zarei Z, Hosseinzadeh A, Kazemi MH, Moradi-Kalbolandi S, Safari E, Farahmand L. Breast cancer: Biology, biomarkers, and treatments. Int Immunopharmacol. 2020;84:106535. doi:10.1016/j.intimp.2020.106535.
2. Wilkinson L, Gathani T. Understanding breast cancer as a global health concern. Br J Radiol. 2022;95(1130):20211033. doi:10.1259/bjr.20211033.
3. Hamdan D, Nguyen TT, Leboeuf C, Meles S, Janin A, Bousquet G. Genomics applied to the treatment of breast cancer. Oncotarget. 2019;10(46):4786–4801. doi:10.18632/oncotarget.27102.
4. Nelson AJO, America GCON. Controversies regarding mammography, breast self-examination, and clinical breast examination. Obstet Gynecol Clin North Am. 2013;40(3):413–427. doi:10.1016/j.ogc.2013.05.001.
5. Kashyap D, Pal D, Sharma R, Garg VK, Goel N, Koundal D, Zaguia A, Koundal S, Belay A. Global increase in breast cancer incidence: Risk factors and preventive measures. Biomed Res Int. 2022;2022:1–16. doi:10.1155/2022/9605439.
6. Fiorica J. Breast cancer screening, mammography, and other modalities. Clin Obstet Gynecol. 2016;59(4):688–709. doi: 10.1097/GRF.0000000000000246.
7. Cserni G, Chmielik E, Cserni B, Tot T. The new TNM-based staging of breast cancer. Virchows Arch. 2018;472(5):697–703. doi:10.1007/s00428-018-2301-9.
8. Fisusi F, Akala E. 2019. Drug combinations in breast cancer therapy. Pharm Nanotechnol. 7(1):3–23. doi: 10.2174/2211738507666190122111224.
9. Haussmann J, Corradini S, Nestle-Kraemling C, Bölke E, Njanang FJD, Tamaskovics B, Orth K, Ruckhaeberle E, Fehm T, Mohrmann S, et al. 2020. Recent advances in radiotherapy of breast cancer. Radiat Oncol. 15(1):71. doi: 10.1186/s13014-020-01501-x.
10. Yin L, Duan J-J, Bian X-W, Yu S-C. 2020. Triple-negative breast cancer molecular subtyping and treatment progress. Breast Cancer Res. 22(1):61. doi: 10.1186/s13058-020-01296-5.
11. Huang Y, Zheng W, Ji C, Wang X, Yu Y, Deng X, Zhou X, Fang L. Circular RNA circRPPH1 promotes breast cancer progression via circRPPH1-miR-512-5p-STAT1 axis. Cell Death Discov. 2021;7(1):376. doi:10.1038/s41420-021-00771-y.
12. Zhao C, Li L, Li Z, Xu J, Yang Q, Shi P, Zhang K, Jiang R. A novel circular RNA hsa_circRPPH1_015 exerts an oncogenic role in breast cancer by impairing miRNA-326-mediated ELK1 inhibition. Front Oncol. 2020;10:906. doi:10.3389/fonc.2020.00906.
13. Li J, Li Y, Cheng H. Circ-RPPH1 knockdown retards breast cancer progression via miR-328-3p-mediated suppression of HMGA2. Clin Breast Cancer. 2022;22(3):e286–e295. doi:10.1016/j.clbc.2021.08.009.
14. Xie J, Ye F, Deng X, Tang Y, Liang J-Y, Huang X, Sun Y, Tang H, Lei J, Zheng S, et al. Circular RNA: A promising new star of vaccine. J Transl Int Med. 2023;11(4):372–381. doi:10.2478/jtim-2023-0122.
15. Yang L, Liu Z, Ma J, Wang H, Gao D, Zhang C, Ma Q. CircRPPH1 serves as a sponge for miR-296-5p to enhance progression of

breast cancer by regulating FOXP4 expression. Am J Transl Res. 2021;13(7):7556–7573.
16. Feng H, Sun S-Z, Cheng F, Zhang N-Q. Mediation of circ_RPPH1 on miR-146b-3p/E2F2 pathway to hinder the growth and metastasis of breast carcinoma cells. Aging (Albany NY). 2021;13(16):20552–20568. doi:10.18632/aging.203439.
17. Yuan Y, Anbalagan D, Lee LH, Samy RP, Shanmugam MK, Kumar AP, Sethi G, Lobie PE, Lim LHK. ANXA1 inhibits miRNA-196a in a negative feedback loop through NF-kB and c-Myc to reduce breast cancer proliferation. Oncotarget. 2016;7(19):27007–27020. doi:10.18632/oncotarget.8875.
18. Kristensen L, Jakobsen T, Hager H, Kjems J. The emerging roles of circRnas in cancer and oncology. Nat Rev Clin Oncol. 2022;19(3):188–206. doi:10.1038/s41571-021-00585-y.
19. Wang P, Qu H, Wang L, Hu Z. Silencing of circUSPL1 represses breast cancer progression by targeting miR-1296-5p/MTA1 axis. Thorac Cancer. 2023;14(22):2198–2209. doi:10.1111/1759-7714.15007.
20. Chen G, He M, Yin Y, Yan T, Cheng W, Huang Z, Zhang L, Zhang H, Liu P, Zhu W, et al. miR-1296-5p decreases ERBB2 expression to inhibit the cell proliferation in ERBB2-positive breast cancer. Cancer Cell Int. 2017;17(1):95. doi:10.1186/s12935-017-0466-y.
21. Xie F, Xiong Y, Yan J, Wang L, Yan W. Circular RNA circ_0048764 promotes the development of breast cancer by regulating microRNA-1296-5p/tripartite motif containing 14 axis. Bioengineered. 2022;13(2):1963–1974. doi:10.1080/21655979.2021.1995990.
22. Qi L, Sun B, Yang B, Lu S. CircRNA RPPH1 facilitates the aggravation of breast cancer development by regulating miR-542-3p/ARHGAP1 pathway. Cancer Biother Radiopharm. 2022;37(8):708–719. doi:10.1089/cbr.2020.4381.
23. Rahman S, Al–Marzouki A, Otim M, Khalil Khayat NEH, Yousuf R, Rahman P. Awareness about breast cancer and breast self-examination among female students at the University of Sharjah: A cross-sectional study. Asian Pac J Cancer Prev. 2019;20(6):1901–1908. doi:10.31557/APJCP.2019.20.6.1901.
24. Salmena L, Poliseno L, Tay Y, Kats L, Pandolfi P. A ceRNA hypothesis: the Rosetta Stone of a hidden RNA language? Cell. 2011;146(3):353–358. doi:10.1016/j.cell.2011.07.014.
25. Chen W, Yu X, Wang N, Jing J, Li R, Lian M. Circ_RPPH1 regulates glioma cell malignancy by binding to miR-627-5p/miR-663a to induce SDC1 expression. Metab Brain Dis. 2022;37(4):1231–1245. doi:10.1007/s11011-022-00965-y.
26. Jia Y, Zhao L-M, Bai H-Y, Zhang C, Dai S-L, Lv H-L, Shan B-E. The tumor-suppressive function of miR-1296-5p by targeting EGFR and CDK6 in gastric cancer. Biosci Rep. 2019;39(1):BSR20181556. doi:10.1042/BSR20181556.
27. Wang L, Hu K, Chao Y, Wang X. MicroRNA-1296-5p suppresses the proliferation, migration, and invasion of human osteosarcoma cells by targeting NOTCH2. J Cell Biochem. 2020;121(2):2038–2046. doi:10.1002/jcb.29438.
28. Xiao F, Ouyang B, Zou J, Yang Y, Yi L, Yan H. Trim14 promotes autophagy and chemotherapy resistance of gastric cancer cells by regulating AMPK/mTOR pathway. Drug Dev Res. 2020;81(5):544–550. doi:10.1002/ddr.21650.
29. Su X, Wang J, Chen W, Li Z, Fu X, Yang A. Overexpression of TRIM14 promotes tongue squamous cell carcinoma aggressiveness by activating the NF-κB signaling pathway. Oncotarget. 2016;7(9):9939–9950. doi:10.18632/oncotarget.6941.
30. Tan Z, Song L, Wu W, Zhou Y, Zhu J, Wu G, Cao L, Song J, Li J, Zhang W. TRIM14 promotes chemoresistance in gliomas by activating Wnt/β-catenin signaling via stabilizing Dvl2. Oncogene. 2018;37(40):5403–5415. doi:10.1038/s41388-018-0344-7.
31. Hu G, Pen W, Wang M. TRIM14 promotes breast cancer cell proliferation by inhibiting apoptosis. Oncol Res. 2019;27(4):439–447. doi:10.3727/096504018X15214994641786.
32. Yao X, Tu Y, Xu Y, Guo Y, Yao F, Zhang X. Endoplasmic reticulum stress-induced exosomal miR-27a-3p promotes immune escape in breast cancer via regulating PD-L1 expression in macrophages. J Cell Mol Med. 2020;24(17):9560–9573. doi:10.1111/jcmm.15367.